

Coupling of magnetospheric cavity modes to field line resonances: A study of resonance widths

Ian R. Mann and Andrew N. Wright

Department of Mathematical and Computational Sciences, University of St. Andrews, Fife
Scotland

Paul S. Cally

Department of Mathematics, Monash University, Clayton, Victoria, Australia

Abstract. By using a box model for the magnetosphere and by using a matrix eigenvalue method to solve the cold linearized ideal MHD equations, we examine the temporal evolution of the irreversible coupling between fast magnetospheric cavity modes and field line resonances (FLRs). By considering the fast mode frequency to be of the form $\omega_f = \omega_{fr} - i\omega_{fi}$, and using a Fourier transform approach, we have determined the full time-dependent evolution of resonance energy widths. We find that at short times the resonances are broad, and narrower widths continue to develop in time. Ultimately, an asymptotic resonance Alfvén frequency full width at half maximum (FWHM) of $\Delta\omega_A = 2\omega_{fi}$ develops on a timescale of $\tau_{fi} = \omega_{fi}^{-1}$. On timescales longer than τ_{fi} , we find that the resonance perturbations can continue to develop even finer scales by phase mixing. Thus, at any time, the finest scales within the resonance are governed by the phase mixing length $L_{ph}(t) = 2\pi(t\delta\omega_A/dx)^{-1}$. The combination of these two effects naturally explains the localisation of pulsations in L shells observed in data, and the finer perturbation scales which may exist within them. During their evolution, FLRs may have their finest perturbation scales limited by either ionospheric dissipation or by kinetic effects (including the breakdown of single fluid MHD). For a continually driven resonance, we define an ionospheric limiting timescale τ_I in terms of the height-integrated Pedersen conductivity Σ_P , and hence derive a limiting ionospheric perturbation scale $L_I = 2\pi(\tau_I d\omega_A/dx)^{-1}$, in agreement with previous steady state analyses. For sufficiently high Σ_P , FLR might be able to evolve so that their radial scales reach a kinetic scale length L_k . For this to occur, we require the pulsations to live for longer than $\tau_k = 2\pi(L_k d\omega_A/dx)^{-1}$. For $t < \tau_k, \tau_I$, kinetic effects and ionospheric dissipation are not dominant, and the ideal MHD results presented here may be expected to model realistically the growth phase of ULF pulsations.

1. Introduction

The coupling of fast magneto-acoustic waves and Alfvén resonances has been an active research topic for many years. This phenomenon is believed to be important for heating solar and laboratory plasmas, as well as being responsible for driving pulsations in the Earth's magnetosphere. It is this last application which we will concentrate on in this paper. Magnetic pulsations are regularly observed by both space-borne and ground-based magnetometers, in the form of ultralow frequency (ULF) waves standing on dipolar field lines. The Doppler signatures of these pulsations are also of

ten observed by HF radar at the ionospheric footpoints of oscillating field lines.

Dungey [1954, 1967] first suggested that pulsations were standing Alfvén waves on dipolar field lines (toroidal modes). He also identified fast poloidal compressional waves, which should propagate across the background magnetic field, and subsequently completed the first decoupled studies of these modes. Southwood [1974] and Chen and Hasegawa [1974] independently presented the first attempts at a full theoretical analysis of the coupled pulsation problem. They proposed that the solar wind, incident upon the magnetospheric cavity and driving magnetosheath flows, could excite a travelling Kelvin-Helmholtz surface wave on the magnetopause. Having an evanescent structure within the magnetosphere, this wave mode could tunnel to excite resonant field line oscillations deep within the magnetosphere. These models however, often require excessively

high magnetosheath velocities to explain the observed pulsations [Hughes, 1994].

Later treatments suggested that global fast modes could be excited throughout the entire magnetospheric cavity in response to sudden impulses in the solar wind [Kivelson et al., 1984; Kivelson and Southwood, 1985]. In this model, standing waves would be set up between the large Alfvén velocity gradient at an outer boundary (often assumed to be the magnetopause) and a turning point within the magnetosphere. The evanescent tail of the modes, beyond the turning point, then drives the Alfvén resonances. This phenomenon has been subjected to much theoretical and numerical modelling [Kivelson and Southwood, 1986; Allan et al., 1986a; Inhester, 1987; Kivelson and Southwood, 1988; Zhu and Kivelson, 1988; Lee and Lysak, 1989; Wright, 1992b] and has been used to predict the frequencies of the cavity mode harmonics, and hence the frequencies of the observed driven nightside/early morning Pc5 Field Line Resonances [Samson et al., 1992a, 1992b; Harrold and Samson, 1992; Walker et al., 1992; Ruohoniemi et al., 1991]. However, a little known paper by Radoski [1976], considered the coupling of cavity modes to Alfvén resonances numerically well before 1985. His early paper predicted many quantitative features which are now well known. His work has many similarities to this paper, and the interested reader is referred to this work.

Recent papers by Wright [1994a], Rickard and Wright [1994, 1995], have considered the propagation of compressional modes down a waveguide. The waveguide models an open magnetospheric cavity where energy can propagate downtail. They conclude that compressional waves, with a low azimuthal wavenumber k_y , will propagate only slowly downtail, while high k_y modes propagate away quickly downtail. These low k_y modes will thus be able to act as long lived and coherent drivers for Alfvén resonances, and hence cavity models, using a small k_y prescription, may still provide a good approximation for modeling coupled pulsation phenomena even when the cavity is open. After all, a waveguide solution may be synthesized from a sum over cavity solutions with suitable k_y values.

Much work has been completed on ULF waves in the Earth's magnetosphere over the last 30 years and readers are referred to the reviews by Southwood and Hughes [1983], Hughes [1983, 1994], and Wright [1994b] for further details. Both the "Kelvin-Helmholtz" and the "cavity/waveguide" mechanisms may be responsible for coupling solar wind energy into ULF pulsations, the dominant one at any time probably depending upon solar wind and magnetosheath conditions. It is probably impossible to explain all data with solely one of these mechanisms.

In the present paper we concentrate upon the cavity model. We use numerical and analytical modeling to address the time-dependent growth of pulsations and the question of field line resonance (FLR) widths.

The latitudinal extent of FLRs is important for two reasons. While Pc 5 pulsations observed by ground-based magnetometers show frequencies corresponding

to theoretically predicted cavity mode frequencies, satellite observations often show several pulsation packets with finite width in L shell, which suggests that they might have been driven by a broadband source, such as a solar wind impulse incident on the magnetosphere. If cavity modes do drive these pulsations, then theory must explain how they can drive Alfvén waves with a finite frequency bandwidth. Satellite observations show that Pc 5 ULF pulsations often occur in spatially (L shell) confined wave packets with typical widths which can be as small as $\sim 0.5R_E$ [Mitchell et al., 1990; Lin et al., 1992]. Magnetometer observations of low-latitude pulsations inside the plasmasphere also found widths as small as $0.2R_E$ [Ziesolleck et al., 1993], which were believed to be driven by tunnelling global modes [Allan et al., 1986b; Zhu and Kivelson, 1989]. Radar measurements of high-latitude FLRs found equatorial resonance widths of $\sim 0.5R_E$ using the STARE radar [Walker et al., 1979], and ionospheric widths of $\lesssim 45$ km, mapping to an equatorial width of $\sim 0.35R_E$, using the Goose Bay HF radar [Walker et al., 1992].

Also, if pulsation scales can narrow to kinetic scale lengths (including where single-fluid MHD breaks down), then mode conversion from the MHD wave mode to kinetic Alfvén or electron inertia waves may occur. Previous numerical models by Inhester [1987] and Rankin et al. [1993] found that kinetic effects could be important within the lifetime of pulsations, and hence excitation of these wave modes might explain observations of auroral arcs which show that their electron precipitation can be modulated at the frequency of a co-existing FLR [Samson et al., 1991, 1992a; Xu et al., 1993]. Walker et al. [1992] show how resonances can be excited so that they take on what they call a "packet structure" in time. Here the amplitude of the resonance grows over several cycles in response to the cavity mode driver, then decays due to dissipation once this forcing is removed. For these kinetic/two-fluid effects to become important, small scales must be reached within the lifetime of this packet.

Pulsations may be damped by a variety of mechanisms, and this can be important both in determining their lifetimes, and in generating finite latitudinal widths. The dominant pulsation energy dissipation mechanism is generally considered to be ionospheric. FLRs drive strong field-aligned currents (FACs) which are closed by Pedersen currents flowing in the ionosphere. These Pedersen currents then damp the pulsations by resistive dissipation at the ionosphere. However, for dayside and active nightside conductivities, this dissipation may be small and allow the FLRs to be relatively long lived ($\sim 10 - 30$ cycles).

Using our numerical model, we investigate both the pulsation energy widths developed by FLRs in space, and whether sufficiently small latitudinal scales can be developed within FLRs so that kinetic effects become important.

The paper is structured as follows: section 2 outlines governing equations and the numerical model; section 3 describes the numerical results and interprets them

using analytic theory. Section 4 discusses the results in relation to observations in the Earth's magnetosphere and section 5 summarizes the paper.

2. Governing Equations and Numerical Model

We now turn to the detailed solution of the coupled ideal MHD wave problem by linearising and assuming that the plasma is cold. We adopt the magnetospheric box model of *Southwood* [1974], and assume that the magnetic field is uniform and lies purely in the \hat{z} direction (See Figure 1). By adopting a density profile $\rho(x)$, we define a continuous Alfvén velocity profile in the \hat{x} (radial or L shell) direction, with the \hat{y} direction completing the triad and representing the azimuthal direction of the dipole magnetosphere.

Assuming that the southern and northern ionospheric boundaries at $z = 0, z_0$ are infinitely conducting, then both displacements ξ_x and ξ_y are zero there (i.e., $\xi(z = 0, z_0) = 0$). Similarly, boundaries in the \hat{x} direction are provided by the large Alfvén velocity gradients at both the magnetopause and the plasmapause. On these boundaries, we impose the condition $\xi_x = 0$, which ensures that waves incident on either of these two boundaries are totally internally reflected, and that wave energy is contained within the box. We assume periodic boundary conditions in the \hat{y} direction, and hence choose displacements to vary as

$$\xi = (\xi_x(x, t), \xi_y(x, t), 0) e^{i\lambda y} \sin k_z z. \quad (1)$$

Here the factor $\sin k_z z$ yields a standing wave solution between the perfectly reflecting northern and southern ionosphere, and λ specifies the azimuthal variation of the waves. With this prescription for ξ , we can derive from the cold linearized ideal MHD equations [e.g., *Boyd and Sanderson*, 1969], the following two coupled differential equations:

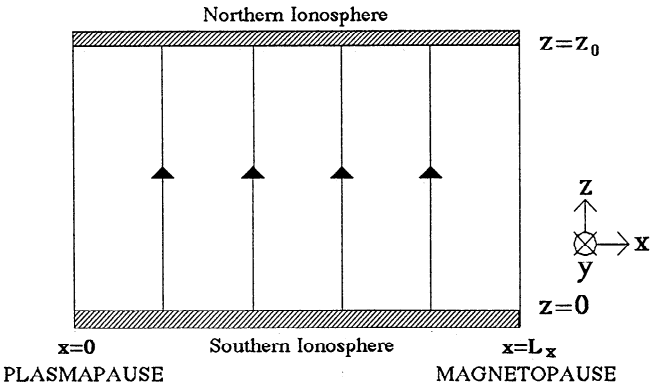


Figure 1. Schematic diagram of the Cartesian box model magnetosphere used in this study. We straighten out the background magnetic field to give a uniform field $B = B_0 \hat{z}$. An inhomogeneous Alfvén speed is obtained in the \hat{x} direction by applying a density profile $\rho(x)$ between $x = 0, 1$. (These boundaries represent the plasmapause and the magnetopause respectively.)

$$\frac{1}{v_A^2(x)} \frac{\partial^2 \xi_x}{\partial t^2} + k_z^2 \xi_x - \frac{\partial^2 \xi_x}{\partial x^2} = i\lambda \frac{\partial \xi_y}{\partial x} \quad (2)$$

$$\frac{1}{v_A^2(x)} \frac{\partial^2 \xi_y}{\partial t^2} + k_z^2 \xi_y + \lambda^2 \xi_y = i\lambda \frac{\partial \xi_x}{\partial x}. \quad (3)$$

If we choose $\lambda = 0$ or ∞ , these two equations decouple [*Dungey*, 1967]. For $\lambda = 0$ they essentially describe the evolution of the fast mode (ξ_x) (equation (2)), and the Alfvén mode (ξ_y) (equation (3)). When $\lambda \rightarrow \infty$, $\xi_y \rightarrow 0$ and ξ_x describes a decoupled poloidal Alfvén wave. When $\lambda \neq 0$ or ∞ , the wave modes are coupled together and energy initially in the fast mode may mode convert to Alfvén wave energy on localized field lines. Asymptotically in time, energy which is initially resident in the fast mode in our model will ultimately reside in narrow resonant Alfvén fields, until it is lost through various dissipation mechanisms [*Radoski*, 1974].

In this model, all lengths are normalized to the magnetopause-plasmapause distance L_x , velocities are normalized to the Alfvén speed in the center of the box, and hence normalized k_z determines the (constant) field line length. We choose a monotonically decreasing $v_A(x)$ profile, defined by

$$v_A^{-2}(x) = A^2 - B^2 \cos(\pi x) \quad (4)$$

so that $x = 0$ represents the plasmapause and $x = 1$ the magnetopause. Consequently, fast cavity modes tend to be confined at high x (the low-density region) and couple to Alfvén resonances positioned at lower x .

To satisfy the boundary conditions on ξ_x in the \hat{x} direction, we write this perturbation as a half-range Fourier sine series [e.g., *Cally*, 1991]

$$\xi_x = \sum_{m=1}^{\infty} a_m(t) \sin(\pi mx). \quad (5)$$

The form of (2) and (3), suggest that ξ_y be expanded in a cosine series,

$$i\xi_y = \frac{1}{2} b_0(t) + \sum_{m=1}^{\infty} b_m(t) \cos(\pi mx). \quad (6)$$

Following a similar procedure to that used by *Cally* [1991] for an incompressible plasma, and assuming a time dependence of $\exp(-i\omega t)$, the coupled equations (2) and (3) can be written as a single generalised matrix eigenvalue problem, as explained in Appendix A. By truncating the expansions to $m \leq N$, the resulting $2N+1$ eigenvalues and associated eigenvectors are used to reconstitute the solution of an initial value problem across the box for all times until energy reaches the finest scale, that is, until a_N or $b_N \neq 0$. This numerical method is novel and has several advantages over more standard finite differencing schemes. Notably, by taking a sufficiently large number of Fourier modes, and following the propagation toward finer scales through the phase mixing process, we can ensure that at any time the structure of the waves is being fully resolved. Our code allows us to compute the resolved wave structures at any time simply by calculating the Fourier summation. This removes the usual finite difference code prob-

lems in calculating long timescale evolutions, whereby the disturbance must be calculated at every previous timestep.

To fully investigate the coupling of magnetospheric cavity modes to FLRs, we choose $\lambda \neq 0$ and take the initial conditions to be the state where only the first ξ_x Fourier mode is excited and at rest, and where no energy resides in the Alfvén continuum (i.e., set $a_1(0) = 1$, $a_{m \neq 1}(0) = 0$ and $b_m(0) = \dot{a}_m(0) = \dot{b}_m(0) = 0$, where \dot{a} denotes da/dt). As the system evolves, energy from this state couples to the Alfvén continuum and excites the field lines resonant with the fundamental fast cavity mode. By varying the parameter λ , the strength of the coupling between the two wave modes is altered, with maximum coupling occurring at some low azimuthal wave number [Kivelson and Southwood, 1986; Zhu and Kivelson, 1988].

We select values of the parameters A^2 , B^2 , and k_z so that only the fundamental fast cavity mode eigenfrequency lies within the Alfvén continuum, defined by $\omega^2(x) = k_z^2 v_A^2(x)$. To do this, we calculated the decoupled ($\lambda = 0$) fast cavity mode eigenfrequencies using a fourth-order Runge-Kutta numerical integration of (2), and used the fact that the cavity mode frequencies remain approximately constant for small changes in λ [Zhu and Kivelson, 1988; Walker et al., 1992; Wright, 1994a].

To check the validity of our code, we followed the temporal evolution of an “energy” invariant. Following Bray and Loughhead [1974], we combine components of the field variables occurring in the linearised, cold MHD equations to yield the magnetic and kinetic energy density terms of the form $\rho_0 \mathbf{v}^* \cdot \mathbf{v}/2$ and $\mathbf{b}^* \cdot \mathbf{b}/2\mu_0$, where \mathbf{v}^* is the complex conjugate of \mathbf{v} . This produced an equation in standard conservation form, that is, $\partial W/\partial t + \nabla \cdot \mathbf{S} = 0$, given by

$$\frac{\partial}{\partial t} \left(\frac{\rho_0}{2} (\mathbf{v}^* \cdot \mathbf{v}) + \frac{(\mathbf{b}^* \cdot \mathbf{b})}{2\mu_0} \right) + \nabla \cdot \left(\frac{\mathbf{b}^*}{\mu_0} \cdot (\mathbf{v} \times \mathbf{B}_0) \right) = 0. \quad (7)$$

No net flux of \mathbf{S} flows out of our model box, and hence using the divergence theorem and integrating over the box volume V gives $\partial/\partial t \int_V W dV = 0$, and hence $\int_V W dV$ is the required invariant. We can hence identify W as the energy density of the waves in our model, and use it to follow the transfer of energy as a function of x from the cavity mode to the FLR in our simulations.

We also checked that the calculated eigenvectors were orthogonal under the weighting of the density profile; that the decoupled ($\lambda = 0$) fast cavity eigenvalues matched those calculated using a fourth order Runge-Kutta shooting algorithm; and using an analogy of our form of the decoupled fast mode equation with Mathieu’s equation [McLachlan, 1947], that the decoupled eigenvectors were calculated correctly.

3. Results

To study how the fundamental cavity mode couples to the Alfvén continuum, we choose normalized param-

eter values of $A^2 = 1.0$, $B^2 = 0.9$, and $k_z = 2.0$. These ensure that the Alfvén resonance occurs well within the magnetospheric box, so that its growth can be studied without the edges of the box significantly altering its structure. With these chosen parameters, the fundamental cavity eigenmode has a normalised angular frequency $\omega \approx 3.574$. Higher harmonic cavity eigenfrequencies lie outside the Alfvén continuum, so that only a single resonance is driven within the box.

3.1. Fast and Alfvén Mode Interaction

For small values of λ , ξ_x and ξ_y are the dominant components for the fast and Alfvén modes respectively and thus provide a useful distinction for discussing our results.

We find that the fundamental cavity mode has approximately 16% of its amplitude in the second Fourier mode, as well as around 1% in the third. Hence its major amplitude component ($\sim 83\%$) corresponds to the fundamental Fourier mode. By imposing the above initial conditions comprising only this Fourier mode, and choosing $\lambda = 1.0$, we can approximate a strongly coupled fundamental cavity eigenmode driver. There will, of course, also be components of higher cavity eigenmodes present which will not be resonantly coupled to the Alfvén continuum.

Figure 2 shows snapshots of the driven ξ_y perturbations at two times. In response to the fast mode driver, a driven field line resonance grows at the expected position ($x \approx 0.22$), where $\omega_A(x) = 3.574$. Figure 2 also shows how the resonance width narrows while the Alfvén oscillations grow in amplitude at the resonant field line. At both of these times, the resonance is already clearly showing a localised structure in x .

To further illustrate this temporal evolution, we use (7) and plot the energy density in the system as a function of both x and time (See Figure 3). The plot shows the growth of the Alfvén resonance in response to the

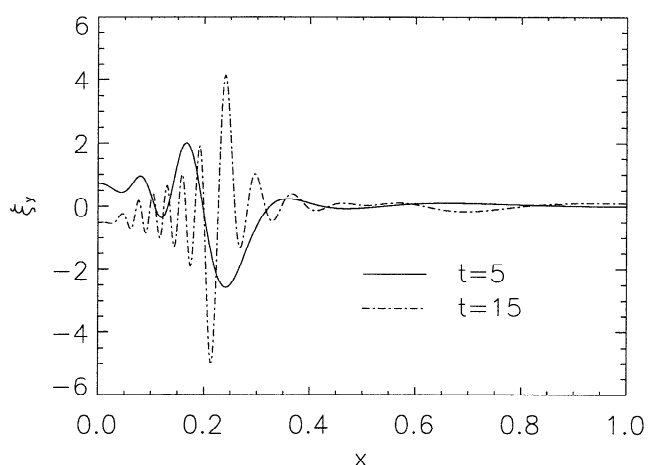


Figure 2. The development of ξ_y perturbations at the resonance in response to the fundamental fast cavity mode driver, for $\lambda = 1.0$. The solid line shows the ξ_y perturbations at $t = 5$, and the dotted-dashed line at $t = 15$. The growth in amplitude and the narrowing of scales in x , due to phase mixing, are clearly shown.

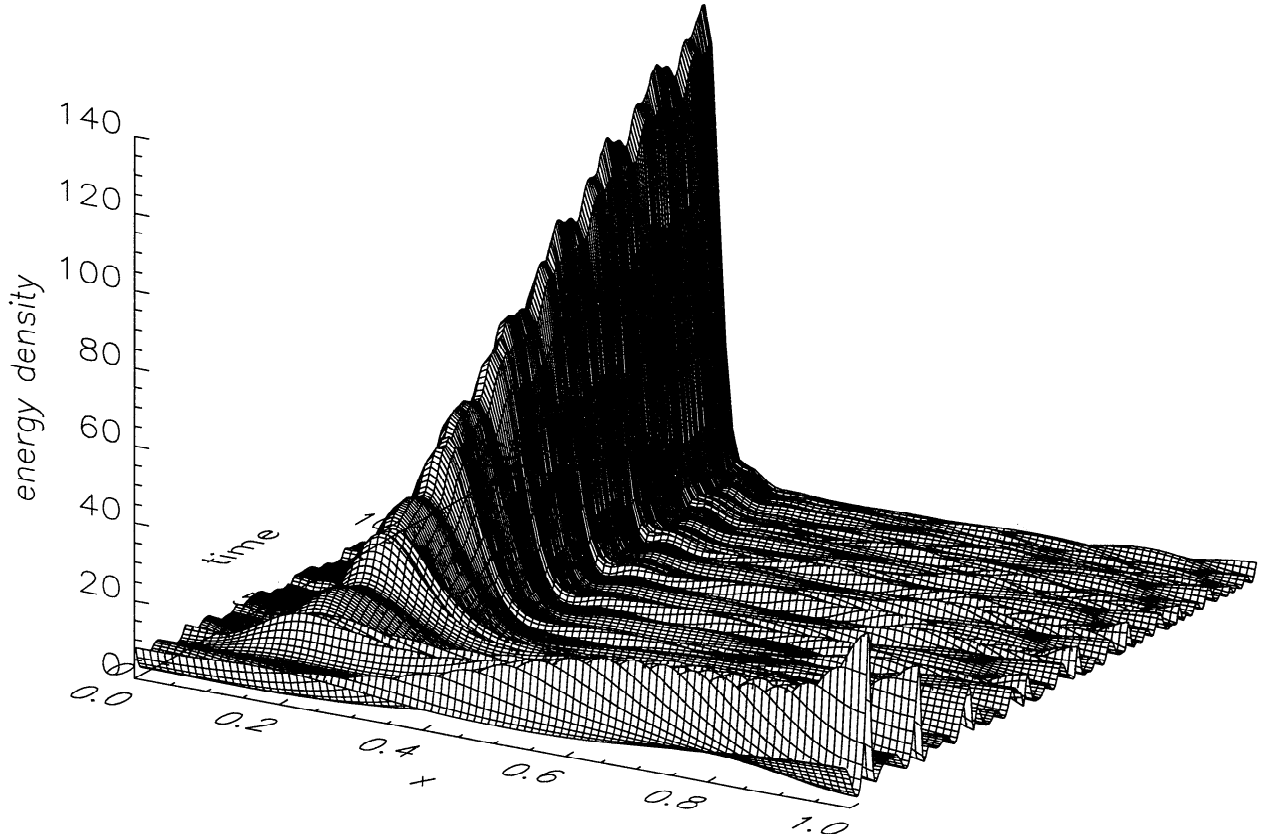


Figure 3. Surface plot of the energy density (arbitrary units) of the wave modes as a function of both x and time (up to $t=15$) for a strong coupling case with $\lambda = 1.0$. The initial fast mode $\xi_x = \sin x$ perturbation sends a fast mode pulse propagating across the box in the x direction. This fast mode energy becomes ducted at large x (in the low Alfvén speed region), but is quickly damped as it drives a large amplitude Alfvén resonance around $x = 0.22$. The energy width of the resonance is seen to narrow in time as it is driven by the fast mode.

initial fast mode. As this system evolves in time, a fast mode pulse propagates backward and forward across the box. This pulse sets up a standing global cavity eigenmode confined to large x , as expected, and both couple energy into the Alfvén resonance.

The energy envelope of the driven resonance is narrow, centered on $x \approx 0.22$, and its width decreases in time. Simultaneously, the amplitude of the fast cavity mode decreases as it is mode converted to Alfvén waves, driving a resonance with increasing amplitude. Ultimately, the resonant amplitude saturates, once all the fundamental cavity mode energy has been transferred. The remaining fast mode energy, confined to large x , continues to oscillate but does not drive FLR's. This remnant fast mode energy represents the proportion of the initial ξ_x Fourier mode which existed in cavity eigenmodes other than the fundamental, and whose eigenfrequencies lie outside the Alfvén continuum.

3.2. Temporal Evolution of Resonance Energy Widths

From Figure 3, it is clear that the energy width of the resonance narrows in time. Previous theoretical studies have concentrated on the expected temporal asymptotic resonance width. Considering the fast mode to have a

complex frequency with an imaginary component ω_{fi} , Southwood and Allan [1987], derived a resonance width

$$\Delta X \sim \omega_{fi} \left(\frac{d\omega_A(x_r)}{dx} \right)^{-1}, \quad (8)$$

where x_r represents the resonance position.

We can continue this analysis further by examining the temporal evolution of this width. Assuming an $e^{-i\omega t}$ dependence, (2) and (3) can be combined to give a single equation for ξ_x

$$\frac{d^2\xi_x}{dx^2} - \lambda^2 \frac{dK^2}{dx} \frac{1}{(K^2 - k_z^2)[K^2 - k_z^2 - \lambda^2]} \frac{d\xi_x}{dx} + (K^2 - k_z^2 - \lambda^2)\xi_x = 0 \quad (9)$$

where $K^2(x) = \omega^2/v_A^2(x)$.

The usual procedure for solving this equation involves adopting a field-aligned wavenumber k_z , which has both real and imaginary components. This has the required effect of removing the singularity and allows for Poynting flux to be driven toward the ionospheres to represent dissipative losses there. Specifying $k_z = k_{zr} + ik_{zi}$ and taking a Taylor expansion of $K^2(x)$ about $(x - x_{res})$, where x_{res} ($= x_r - i\epsilon$) is defined by $K^2(x_{res}) = k_z^2$ and

represents the resonance position, then (9) can then be written (in the vicinity of the resonance) as [Southwood, 1974; Rankin *et al.*, 1993],

$$\frac{d^2\xi_x}{dx^2} + \frac{1}{(x - x_r + i\epsilon)} \frac{d\xi_x}{dx} - \lambda^2 \xi_x = 0 \quad (10)$$

where

$$\epsilon = -2k_{zr}k_{zi}/(dK^2(x)/dx) \quad (11)$$

and x_r represents the resonance position on the real x axis.

A problem exists with this formulation, as noted by Kivelson and Southwood [1988]: the field-aligned currents of an Alfvén wave are closed by Pedersen currents in the ionosphere, and thus k_{zi} is determined by Σ_P , the height-integrated Pedersen conductivity. The fast mode interacts with the ionosphere in a different fashion to the Alfvén wave, typically being better reflected and having a smaller k_{zi} . Thus a problem arises in a coupled fast-Alfvén wave solution; it is impossible to choose a single value for k_{zi} which is appropriate near the resonance (dominated by Alfvénic perturbations), and away from the resonance (dominated by the fast mode). In the literature, k_{zi} is chosen to be that corresponding to the Alfvén wave in all studies we are aware of.

Alfvén waves naturally drive field-aligned currents, and by imposing an imaginary k_z the damping of these Alfvén waves by currents flowing in the resistive ionospheres can be readily modeled. However, imposing the same boundary conditions on the fast mode waves forces them to similarly drive large Pedersen currents. This would cause the fast modes to become damped directly by Joule dissipation, when in fact they should not be significantly damped by this mechanism. This is because the Pedersen currents driven by the fast modes are several orders of magnitude less than those driven by Alfvén waves. In fact, the fast mode electric field should be subject to the boundary condition $E_M \approx 0$, where E_M represents the wave electric field at the ionosphere [Kivelson and Southwood [1988]].

In order to avoid potentially unrealistic effects, we choose to adopt a more physical picture for “damping” the fast mode. In an entirely analogous way, we choose to remove the singularity in (9) by adopting a complex frequency rather than a complex k_z . This represents the oscillating cavity mode naturally, which is decreasing in amplitude as it couples to the Alfvén resonance (cf. the quasi-modes)[Barston, 1964; Sedláček, 1971]. If we assume that $K^2(x)$ is complex, because of the complex cavity mode frequency, we can write

$$\omega_f = \omega_{fr} - i\omega_{fi}, \quad (12)$$

with the negative sign so that the $e^{-i\omega t}$ dependence “damps” the cavity mode. This assumes that the entire fast mode will decay uniformly as it drives the Alfvén resonance, which should be a particularly good approximation when λ is small [Wright, 1992a]. This then gives (10), with the damping now defined by

$$\epsilon = \frac{-2\omega_{fi}\omega_{fr}}{v_A^2(x)(dK^2(x)/dx)}. \quad (13)$$

With this approach, the cavity mode is damped due to coupling to the Alfvén resonance rather than direct ionospheric dissipation. We can hence consider that the width of the Alfvén resonance, in the absence of ionospheric dissipation, will be determined by which field lines the cavity mode actually drives.

To calculate the temporal evolution of this resonance width, we can hence examine the frequency bandwidth of the driver at any time τ_0 by taking the Fourier transform of the ξ_x time history, to give $F(\omega)$ [Bracewell, 1986]. To remove the phase effects of $F(\omega)$, we can consider the bandwidth of the driver in terms of energy or power (i.e., in terms of displacements squared). We can thus write

$$P(\omega) = [F(\omega)]^* F(\omega) = \xi_0^2 \times \frac{1 + e^{-2\omega_{fi}\tau_0} - 2e^{-\omega_{fi}\tau_0} \cos[(\omega_{fr} - \omega)\tau_0]}{[\omega_{fi}^2 + (\omega_{fr}^2 - \omega^2)]} \quad (14)$$

where $[F(\omega)]^*$ represents the complex conjugate of $F(\omega)$. Hence we have an analytic expression for the frequency spectrum in energy of the driving fast cavity mode.

Two different width regimes exist for the function $P(\omega)$: 1) short times ($\tau_0 \ll 1/\omega_{fi}$)

$$P(\omega) = \frac{4\xi_0^2}{[\omega_{fi}^2 + (\omega_{fr} - \omega)^2]} \sin^2\left[\frac{(\omega_{fr} - \omega)}{2}\tau_0\right]. \quad (15)$$

If $\omega_{fr} \gg \omega_{fi}$ then

$$P(\omega) \simeq \xi_0^2 \tau_0^2 \text{sinc}^2\left(\left(\frac{\omega_{fr} - \omega}{2}\right)\tau_0\right) \quad (16)$$

where the sinc function (familiar from Fourier optics) is defined by $\text{sinc}(x) = \sin(x)/x$; 2) asymptotic times ($\tau_0 \gg 1/\omega_{fi}$)

$$P(\omega) = \frac{\xi_0^2}{[\omega_{fi}^2 + (\omega_{fr} - \omega)^2]}. \quad (17)$$

This is a Lorentzian profile, and has a full width at half maximum (FWHM) of $\Delta\omega = 2\omega_{fi}$.

In terms of the above analysis, the energy width of the resonance region will be determined by the frequency bandwidth of $P(\omega)$. By calculating the FWHM frequency bandwidth $\Delta\omega$ at any time τ_0 , we can predict the physical energy width of the resonance ΔX_E at this time using the relation

$$\Delta X_E(\tau_0) = (\Delta\omega(\tau_0)/\omega_A'(x_r)) \quad (18)$$

where $' = d/dx$.

Considering the spectrum of individual plasma displacements by taking the square root of $P(\omega)$, suggests that the asymptotic FWHM of the FLRs, seen in terms of their fields, will be a factor of $\sqrt{3}$ greater than ΔX_E . We can denote this length by L_{fi} . This differ-

ence between perturbation and energy FWHM can be seen clearly in our numerical results, shown later.

Consequently, we can predict the temporal evolution of ΔX_E which we expect to see in our numerical model. We do this by solving the transcendental equation for $\Delta\omega$ using the function $P(\omega)$, inserting the value of ω_{fr} (the fundamental cavity mode eigenfrequency, calculated using the Runge-Kutta routine) and a value for ω_{fi} .

Using the approximation that all fast mode oscillations can be described by a single complex frequency (see equation (12)), and energy conservation, we infer that the Alfvén energy (calculated on the basis of $\rho\xi_y^2/2 + b_y^2/(2\mu_0)$), integrated across the entire magnetospheric box, would grow as

$$E_A(t) = E_{A0}(1 - \exp(-2\omega_{fi}t)). \quad (19)$$

Consequently, plotting $\ln\{[E_{A0} - E_A(t)]/E_{A0}\}$ against t , allows ω_{fi} to be calculated from the gradient.

The width calculated by the above ad hoc method, ΔX_E , can then be compared to the widths measured directly from the results of the numerical solution (see Figure 4). In this figure, we plot as solid lines the overall energy width of the resonance measured using the results from our numerical code, and show the width evolution which we expect on the basis of this Fourier analysis as dashed lines. Figure 4 clearly shows how this energy width decreases as time evolves and ultimately saturates to a constant value determined by the damping rate of the fast cavity mode.

It is clear that this simple analysis, whereby we assume that the energy width of the resonance is governed by the frequency bandwidth of the driver, matches our

numerical results excellently. This is a new result, which predicts that the overall widths in L shell of pulsations in the Earth's magnetosphere will evolve and narrow in time. Satellites crossing these L shells should observe relatively broad resonances soon after a cavity mode has started to deposit its energy at the resonance. Observations of well-established FLRs, long after the cavity mode has driven the resonance, should have a narrower saturated width given by (17). As stated above, these asymptotic widths will be determined by the damping rate of the cavity mode, which in the real magnetosphere will depend not only on their coupling rate to Alfvén waves (in our model governed by ω_{fi}) but also other cavity mode losses such as propagation downtail, into the polar cap, or out through nonperfectly reflecting boundaries such as the magnetopause.

We believe that analysis using this procedure can give valuable insight into why resonances adopt specific widths and perhaps provide an important analytic tool when considering the various driving mechanisms which have been proposed for exciting magnetospheric pulsations.

3.3. Fast Cavity Mode Coupling Rates

Clearly, with our box model for the magnetosphere and within the framework of ideal MHD, the loss of energy from the cavity mode occurs only as a result of coupling to an Alfvén resonance. In a realistic magnetosphere, with additional fast mode energy losses, ω_{fi} may be slightly larger than the value adopted here. Once a suitable value of ω_{fi} has been estimated, the frequency bandwidth of the fast mode is determined. Consequently, this coupling rate has an important role to play in determining the energy widths adopted by resonances.

Using the method for obtaining ω_{fi} previously described, we can follow Kivelson and Southwood [1986] and Zhu and Kivelson [1988] and plot ω_{fi} versus the parameter $\lambda^2/\omega^{4/3}$ (we choose this parameter as our ordinate to facilitate comparison with previous studies which assumed a linear density profile and where a transformation to yield Budden's [1961] equations generates the variable $\lambda^2/\omega^{4/3}$. See also Forslund et al. [1975]). For our study, we find that the maximum coupling rate occurs when our normalized (dimensionless) $\lambda = \lambda_{max} = 1.6$, which corresponds to $\lambda^2/\omega^{4/3} \approx 0.5$ (see Figure 5). This gives a damping of $\omega_{fi}/\omega_{fr} = 0.06$, which means that the fast mode would damp on a timescale $\tau_{fi} = 2.65$ periods. This is encouraging as it means that resonances excited by this rapidly damped fast mode can develop narrow overall energy widths on the timescale of a few driving periods, as was suggested necessary by Walker et al. [1992].

Zhu and Kivelson [1988] found that using their box geometry with density proportional to x the maximum coupling occurred when the parameter $\lambda^2/\omega^{4/3} = 0.5$. Qualitatively our results agree well with their analysis (any differences being attributable to the different density profiles). In the hemicylindrical model of Al-

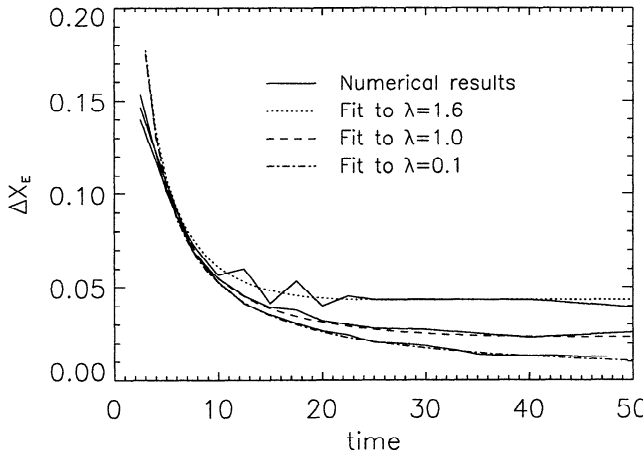


Figure 4. Temporal evolution of FLR energy widths. As time evolves, the energy width of the resonances ΔX_E in space is seen to narrow due to phase mixing, and asymptotically approaches the width due to the damping rate of the driving fast mode ω_{fi} . The solid lines show the widths as measured from the results of our numerical solution, and the dashed lines show the fit to these results based on our Fourier analysis where we assume the driving fast mode to have the form $\xi_x = \xi_{x0} \exp[-i(\omega_{fr} - i\omega_{fi})t]$.

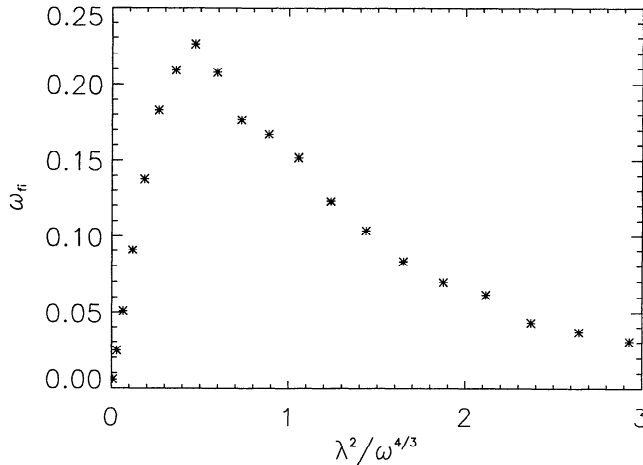


Figure 5. Coupling strength of the fast and Alfvén wave modes. We measure the coupling rate of the fast mode by ω_{fi} , and plot it against the parameter $\lambda^2/\omega^{4/3}$ using the results from our numerical code. Maximum coupling occurs where $\lambda \approx 1.6$. The coupling strength decreases on either side of the maximum giving the asymptotic decoupled limits at $\lambda = 0, \infty$.

lan et al. [1986a], the maximum coupling occurred when their dimensionless $m \approx 3$. This is of the same order as our dimensionless $\lambda_{max} = 1.6$.

3.4. Phase Mixing Lengths

From the analysis in the previous section, it is clearly possible for cavity modes to drive FLRs with a finite width in L shell, encompassing resonant field lines with a range of natural Alfvén frequencies, as seen in satellite data [Mitchell et al., 1990; Lin et al., 1992].

It is well known that the coupling of fast and Alfvén MHD wave modes has many analogies to the behavior of a classical driven harmonic oscillator (see Wright [1992b] and Steinolfson and Davila [1993] for the case of cavity modes excited in solar coronal loops). Consequently, exactly on resonance where the real part of the cavity mode frequency matches the local Alfvén frequency ($\omega_{fr} = \omega_A(x)$), we expect to observe monotonic growth of Alfvén oscillations on a timescale of $\tau_{fi} = \omega_{fi}^{-1}$. Off resonance, however (but still within $\Delta\omega$), we expect a beating Alfvén wave response due to the frequency mismatch between the cavity mode and the now slightly different natural Alfvén frequency of this particular field line. On timescales longer than τ_{fi} , once the driving cavity mode has decayed, the Alfvén oscillations should then settle down to vibrate with their own natural frequency $\omega_A(x)$ [Allan and Poulter [1989]].

Figure 6 reproduces this expected behaviour both on and just off-resonance using our numerical model. This response compares well with the previously published results of Allan and Poulter [1989] and Wright [1992b] for the magnetospheric case and those of Poedts et al. [1990] and Steinolfson and Davila [1993] for the coronal loop case.

As a consequence of the inhomogeneous background natural Alfvén frequency in the \hat{x} direction, then we

can expect the perturbations within these radial pulsation packets, which are initially excited in phase, to drift out of phase with each other in time. This process is called phase mixing [Burghes et al., 1969; Heyvaerts and Priest, 1983]. Phase mixing continually reduces the scale length of the disturbance in time, and we can define the length scale reached after a time t as the phase mixing length $L_{ph}(t)$.

Considering an ideal solution of the form

$$\xi_y(x, t) = A(x) \exp[i\omega_A(x)t] \quad (20)$$

and assuming that $\partial/\partial y = 0$, we can differentiate with respect to x to gain the local wavenumber $k_x(x)$. This then gives $k_x(x) \approx \omega'_A(x)t$ (where prime denotes d/dx) and allows us to define

$$L_{ph}(t) = 2\pi [\omega'_A(x)t]^{-1}. \quad (21)$$

Although the decoupled oscillation of each field line relies upon $\partial/\partial y = 0$, we shall see from our numerical model, that even when $\partial/\partial y \neq 0$ the scale length of the solution in x is still dominated by the decoupled phase mixing length. This continual narrowing of spatial scales in time can be thought of as a wave propa-

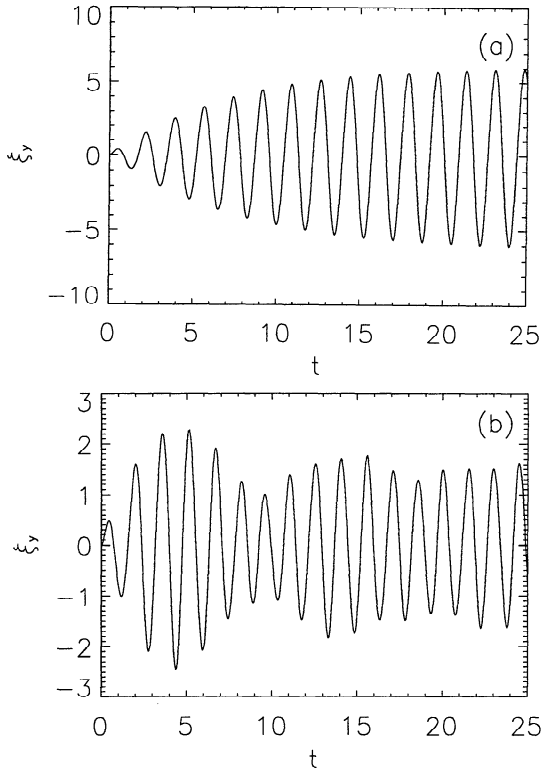


Figure 6. Growth of ξ_y perturbations in time. (a) the growth of the ξ_y fields exactly on resonance, at the position $x = 0.22$ for $\lambda = 1.0$, which represents a quite strong coupling case. The resonant amplitude grows smoothly to a maximum value which is attained once all the fundamental cavity mode energy has been transferred to the resonance. (b) The off resonance behaviour, again for $\lambda = 1.0$, showing the expected beating between the driving cavity mode frequency ω_{fr} and the natural Alfvén frequency $\omega_A(x)$, here at $x = 0.17$.

gating in modenumber space toward higher harmonics. Cally [1991] considered the speed of propagation of the outermost wavefront in this mode number space for an incompressible plasma, and the concept is discussed in greater detail in the work by Cally and Sedláček [1994].

As finer scales develop, the Alfvén oscillations (ξ_y), develop very high gradients of $\partial \xi_y / \partial x$, associated with very strong field aligned-currents j_z given by

$$\begin{aligned} j_z &= \frac{(\nabla \times \hat{\mathbf{b}})_z}{\mu_0} = \frac{1}{\mu_0} \left(\frac{\partial b_y}{\partial x} - \frac{\partial b_x}{\partial y} \right) \\ &= \frac{B_0 k_z \cos k_z z}{\mu_0} \left(\frac{\partial \xi_y}{\partial x} - i\lambda \xi_x \right), \end{aligned} \quad (22)$$

where $\mu_0 = 4\pi \times 10^{-7} \text{ NA}^{-2}$.

Figure 7 shows snapshots of the spatial structure of the energy density, the resonant Alfvén perturbation described by ξ_y , and the derived field-aligned current for two chosen values of λ at one single time, $t = 45$.

The first column in Figure 7 shows results for a small value of λ (here taken as 0.1), where $t < \tau_{fi} \approx 330$.

The system evolves so that at this time, the resonance energy width ΔX_E is small and of the order of L_{ph} , as are the perturbation scales within the resonance. An almost singular resonance is excited with little obvious fine ξ_y structure visible beneath the energy envelope. This compares well with the full nonlinear FLR resonance width results published by Rankin et al. [1993]. In their model, they drive resonances with a ramped and then constant amplitude incident fast mode. We would expect this driver to be almost monochromatic and drive a very narrow resonance. Some small finite width is developed in their scheme due to dissipation and non-linear processes which they included in their numerical code.

The second column of Figure 7, on the other hand, shows perturbations excited with a rather larger value of $\lambda = 1.0$, where $t > \tau_{fi}(\lambda) = 7$. In this case, the anticipated j_z and ξ_y fine scale spatial oscillations are clearly seen beneath the now much broader energy envelope ΔX_E .

We can now see why the perturbations show the two types of behavior seen in Figure 7. For small coupling

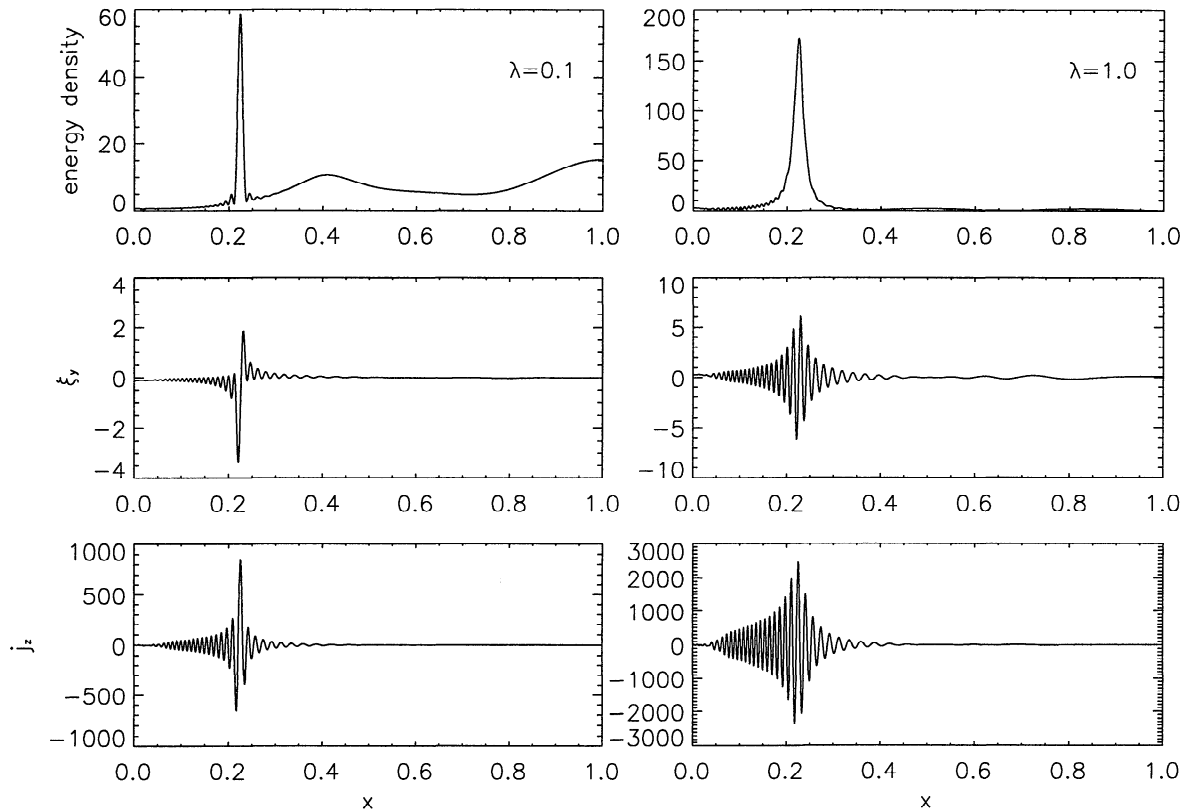


Figure 7. Energy density, ξ_y perturbation and j_z as a function of x at the time $t = 45$. Left Column: The $\lambda = 0.1$ case, where the coupling of the fast and Alfvén modes is weak. For this case $t < \tau_{fi} \approx 330$. We can see that significant energy still resides in the fast mode at high x , and that both the energy and ξ_y have similar narrow widths governed by the phase mixing length (L_{ph}). Strong field aligned currents j_z have already been established at this time. Right column: The $\lambda = 1.0$ case, representing stronger coupling. This is a case where $t > \tau_{fi} \approx 7$. Here the energy width is broad and has saturated at the asymptotic width. However, the ξ_y perturbations have continued to develop fine scales through phase mixing and these are apparent inside the energy envelope. In the case shown in this second column, more energy has been transferred to the resonance and it has driven extremely strong field aligned currents (FAC's).

rates (here the $\lambda = 0.1$ case), the value of ω_{fi} is small, and the time $\tau_{fi}(\lambda)$ is large (~ 330). Consequently, the energy envelope is still narrowing at $t = 45$ and has a width of order the phase mixing length.

For the stronger coupling rate, shown in the second column of Figure 7 ($\lambda = 1.0$), the energy width ΔX_E is wide, and this is reached in the now short time $\tau_{fi}(\lambda) \approx 7$. Now, $t \gg \tau_{fi}$, and the phase mixing length L_{ph} is much smaller than the overall pulsation width. Consequently, fine structure is revealed inside the resonance envelope.

If magnetospheric pulsations have lifetimes longer than τ_{fi} , they have time to evolve (phase mixing) fine structure within their energy envelope. Realistic spatial pulsation packets in the magnetosphere may contain several spatial oscillations and satellites crossing these pulsation packets might see oscillations from both crossing oscillations in space, as well as the temporal oscillation of the field lines (cf. the AMPTE/CCE results of *Anderson et al.* [1989]).

Ideal phase mixing means that the ξ_y perturbation scales continually narrow in time. Following *Cally* [1991], we can plot a diagram of the magnitude of the coefficients b_m (i.e., the ξ_y Fourier amplitudes) as a function of time. In the incompressible work of *Cally* [1991] a clear pulse of energy was seen propagating in wave number space toward higher Fourier harmonics (and hence smaller spatial scales) in time. Figure 8 shows the magnitude of the coefficients b_m at two times, and a similar (if less smooth) picture of this propagation is revealed for the ξ_y components in our compressible case. We can estimate the finest scales which may be generated by phase mixing by considering the maximum magnitude of the natural Alfvén frequency gradient $|\omega'_A|_{max}$, and then using

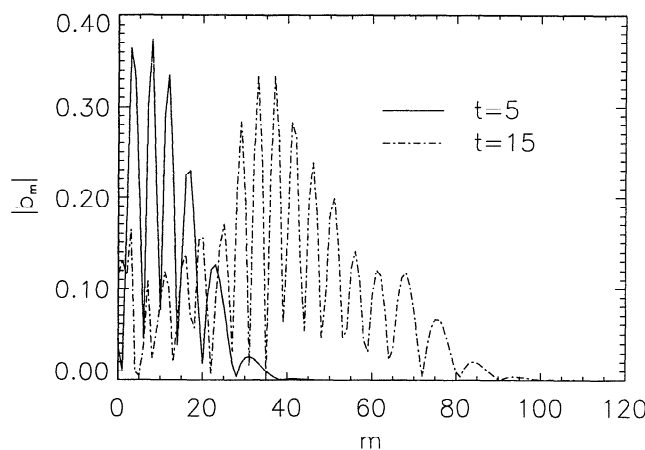


Figure 8. The magnitude of the components $b_m(t)$ in the Fourier series expansion for $\xi_y = b_0(t)/2 + \sum_{m=1}^N b_m(t) \cos(\pi mx)$, plotted at two times, for $\lambda = 1.0$. We can clearly see a wave pulse propagating in wavenumber space (m) towards higher harmonics and hence finer scales, due to phase mixing. The solid line represents an early time ($t = 5$) and the dashed line a later time ($t = 15$).

$$k_{x,max} = m_{max}\pi = |\omega_A'|_{max} t \quad (23)$$

to give

$$m_{max} = \frac{1}{\pi} |\omega_A'|_{max} t. \quad (24)$$

This predicts an increase in m between two times as $\Delta m = (|\omega_A'|_{max})\Delta t$. Hence between $t=5$ and 15 , the foremost wavefront should advance by a Δm of 51, in good agreement with the results shown in Figure 8.

In the real magnetosphere, pulsations can be damped by a variety of mechanisms, such as ohmic dissipation in the ionosphere. This can damp the pulsation, as well as creating finite widths. If pulsations generate sufficiently fine scales in space, then they can mode convert to kinetic or two fluid wave modes which may broaden the resonance [*Rankin et al.*, 1993]. These dissipation mechanisms may limit the extent to which realistic pulsations will phase mix and hence limit the finest radial scales which they will develop. We discuss these effects and compare our results to other studies in the following sections.

4. Discussion

4.1. Overall Pulsation Energy Widths

We can now compare the asymptotic resonance widths (ΔX_E) developed in our numerical model with the overall pulsation widths which have been observed in the terrestrial magnetosphere.

We use (18) and follow *Anderson et al.* [1989, and references therein] by adopting their dipole magnetic field geometry. By assuming fast mode damping parameter of $\omega_{fi}/\omega_{fr} = 0.06$ (to illustrate a typical coupling strength), then we expect the asymptotic values of ΔX_E to be $\sim 0.2R_E$ at $L = 4$ (assumed to be inside the plasmasphere), and at $L = 7$ (in the outer magnetosphere) $\sim 0.4R_E$. For a less strongly coupled cavity mode, these widths would be reduced.

Resonance widths seen in radar data are of $\sim 0.5R_E$ [*Walker et al.*, 1979] and $\sim 0.35R_E$ [*Walker et al.*, 1992]. *Walker et al.* [1992] note that their observation was at the limiting ionospheric resolution of their radar (~ 45 km) and hence that the real width of the FLR which they observed could have been narrower than the inferred width of $\sim 0.35R_E$. Similarly, the satellite observations of *Mitchell et al.* [1990] showed pulsations (which they believed to have been driven by a cavity mode) with a width of $\sim 0.5R_E$. These widths are clearly of the order predicted by our numerical code.

4.2. Magnetospheric Perturbation Widths ΔX_ξ

We now discuss the likely dominant damping mechanisms for magnetospheric pulsations. By considering this damping, we can determine whether pulsations are sufficiently long lived that the phase mixing structure within the energy envelope can develop.

Allan and Poulter [1989] concluded that it would take approximately hundreds of periods or more for dissipation

pative phase mixing to damp out magnetospheric pulsations. Consequently, it is unlikely to be an important pulsation damping mechanism. Kelvin-Helmholtz instabilities can be driven in regions of high-velocity shear, which may be generated by phase mixing within Alfvén resonances. These instabilities could be important for both widening the resonance region and for damping the pulsations. However, this will be a non-linear effect, so is not present in our linear analysis. (See *Browning and Priest* [1984] for a discussion of the Kelvin-Helmholtz stability of phase mixed Alfvén wave fields.)

The dominant mechanism for dissipating pulsation energy is usually regarded as ionospheric Joule heating. The energy dissipated by this mechanism clearly depends on the conductivity of the ionosphere, which is modeled using the height-integrated Pedersen conductivity Σ_P of the assumed thin sheet ionosphere.

We have discussed the different ionospheric boundary conditions which are applicable to decoupled cavity modes and Alfvén waves. We have argued that even for coupled modes, assuming two different boundary conditions provides a good approximation, and hence that the overall width of an FLR can be understood in terms of the frequency bandwidth of the cavity mode rather than being due to direct ionospheric dissipation.

However, once the Alfvén waves have been driven by the cavity mode, they have a finite lifetime based on this ionospheric damping. To incorporate the effects of ionospheric dissipation into our dynamic analysis in terms of phase mixing, we can consider the following theory.

4.2.1. Steady state analysis. The standard treatment in the literature for the case of continually driven pulsations finds the standard steady harmonic solution to the coupled wave problem by considering a single complex k_z ($\omega_{fi} = 0, k_{zi} \neq 0$). The leading order solution for ξ_x modes can be written as [*Southwood*, 1974]

$$\xi_x \sim \ln(\lambda(x - x_r + i\epsilon)). \quad (25)$$

Writing down the leading order solution for the ξ_y (i.e., Alfvén wave) resonant response, then we obtain

$$\xi_y \sim \frac{1}{\lambda(x - x_r + i\epsilon)}. \quad (26)$$

Considering this function, we can write

$$|\xi_y| \sim \frac{1}{\lambda((x - x_r)^2 + \epsilon^2)^{\frac{1}{2}}} \quad (27)$$

and derive a perturbation FWHM ΔX_ξ of

$$\Delta X_\xi = 2\sqrt{3}\epsilon \quad (28)$$

where ϵ is calculated using a complex k_z based simply on ionospheric dissipation (see equation (11)). *Ellis and Southwood* [1983] show that for $v_A \gg (\mu_0 \Sigma_P)^{-1}$ (as is appropriate for the Earth), then

$$k_i \approx \frac{2}{\mu_0 \Sigma_P v_A z_0}. \quad (29)$$

We expect that a time-dependent solution will asymptote to this width for large times, and now demonstrate how our dynamic analysis in terms of phase mixing may reproduce this result.

4.2.2. Phase mixing analysis. A steadily driven resonance ($\omega_{fi} \approx 0$) is best simulated in our model by a weak coupling case, $\lambda \rightarrow 0$. We choose to adopt a dynamic viewpoint of this situation in terms of a superposition of Alfvén waves: Alfvén waves with relatively large amplitude and spatial scale in x are continually being driven. The Alfvén waves excited at a given time will phase mix more and more the longer they live; however, they also decay in amplitude and so become more insignificant. Thus ionospheric dissipation limits the finest scales that can be achieved for significant amplitudes. If we assume that after an e-fold damping time τ_I (due to ionospheric dissipation) the Alfvén wave amplitude is no longer significant, we can determine the finest scales which the pulsation can develop. This is given by the limiting ionospheric phase mixing length, L_I

$$L_I \sim 2\pi[\tau_I \omega_A'(x)]^{-1}. \quad (30)$$

We can now write

$$\tau_I \sim 1/\gamma = \frac{\Sigma_P \mu_0 z_0}{2} \quad (31)$$

where γ represents the ionospheric damping rate of an undriven Alfvén wave component, and hence

$$\Delta X_\xi \approx L_I \sim 2\pi \left(\frac{\Sigma_P \mu_0 z_0}{2} \omega_A'(x) \right)^{-1}. \quad (32)$$

This predicts the finest wave scales which develop in a steadily driven pulsation to be $\propto [\Sigma_P z_0 \omega_A'(x)]^{-1}$.

The steady harmonic ($\omega_{fi} = 0, k_{zi} \neq 0$) estimate for the resonance width of ξ_y from the previous subsection (equations (28), (11), and (29)) gives

$$\Delta X_\xi = 2\sqrt{3} \left(\frac{\Sigma_P \mu_0 z_0}{2} \omega_A'(x) \right)^{-1}. \quad (33)$$

Again this clearly results in $\Delta X_\xi \propto [\Sigma_P z_0 \omega_A'(x)]^{-1}$. This analysis shows how our novel dynamic phase mixing treatment can reproduce more standard steady harmonic results. The two results differ by a factor ~ 2 , but this is not totally unexpected because of the order of magnitude estimate of the ionospheric e-fold damping time. It is encouraging that our treatment, based on phase mixing, reproduces the expected result that ionospheric damping will limit the finest ξ_y perturbation scales which may be developed by a continually driven resonance.

4.3. Pulsation Characteristics

We can also consider the effects of ionospheric dissipation on FLRs driven by single damped cavity modes

(i.e., with $\omega_{fi} \neq 0$). If $\tau_I > \tau_{fi}$, then this introduces the possibility that FLRs have fine phase mixing structure inside their overall width.

Fine scales which are created within a pulsations energy envelope will continue to narrow by phase mixing, whilst their amplitude decreases due to ionospheric dissipation. If the Alfvén waves gain their energy on timescales which are quick compared to τ_I , that is, $\tau_I \gg \tau_{fi}$, then we can view the pulsation in two stages: the first, for times of order τ_{fi} , is essentially the ideal growth of the resonance; the second ($t \gg \tau_{fi}$) represents the undriven phase mixing decay of Alfvén waves. Hence we can calculate an ionospheric pulsation damping rate by considering the decay of undriven Alfvén waves. For FLRs driven by rapidly damped cavity modes, this should be reasonably accurate.

A numerical calculation of this ionospheric damping rate, in a dipole magnetospheric geometry, was completed by *Newton et al.* [1978]. They found that for typical dayside (or active nightside) Σ_P , the damping decrement $\gamma/\omega_{Ar} \sim 0.01$ (see, for example, their Figure 9, with $L = 7$ and $\Sigma_P = 10\text{-}20$ mhos ($9 \times 10^{12} - 1.8 \times 10^{13}$ esu); they calculate $\gamma/\omega_{Ar} \sim 0.0075 - 0.018$). If we define the e-fold ionospheric damping time of the pulsations as τ_I , then this value of γ/ω_{Ar} corresponds to $\tau_I = 15.9$ Alfvén wave periods. This is longer than τ_{fi} for pulsations driven by strongly coupled fast cavity modes, and therefore we would expect these dayside pulsations to develop the phase mixing fine structure within the resonance envelope. Similarly, using typical nightside conductivities of $\Sigma_P \sim 0.1\text{-}1$ mho ($\sim 10^{11} - 10^{12}$ esu), *Newton et al.* [1978] found damping on the nightside can become extreme, having $\gamma/\omega_{fr} \gtrsim 0.1 - 1$. Clearly, this is probably not sufficient for perturbation fine structure to develop significantly beneath the pulsations energy envelope, even for rapidly damped cavity modes.

Consequently, satellites crossing dayside or active nightside FLRs may see oscillations in magnetic field components both from it going through spatial oscillations, as well as seeing the natural Alfvén oscillations of the local field lines in time. This implies that inbound and outbound satellites, which are crossing FLR's, may see different apparent frequencies. Frequency shifts of this form were seen in the AMPTE/CCE data presented by *Anderson et al.* [1989].

If $\tau_I \lesssim \tau_{fi}$, as is the case for the non-auroral region nightside, then pulsation fine structure of significant amplitude will not be created within the overall resonance envelope and pulsations will be rapidly damped by ionospheric dissipation. However, *Crowley et al.* [1987], used both EISCAT radar and ground-based magnetometer data from observations of a Pc 5 pulsation to determine both its observed damping decrement and a theoretically predicted damping rate calculated on the basis of ionospheric dissipation. Σ_P ($\sim 2 - 5$ mho) was inferred from the EISCAT data and predicted damping greater than that observed. *Crowley et al.* [1987] argued that the FLRs amplitude was being enhanced by a cavity mode continuing to drive

it during the period of observation. This would be a case where $\tau_I \lesssim \tau_{fi}$, and explains how pulsations with short τ_I may have longer lifetimes than those predicted on the basis of τ_I alone.

For sufficiently long lived pulsations, then phase mixing can narrow to kinetic/two-fluid length scales L_k (such as the ion gyroradius, or the electron inertia length). These effects will become important, from a phase mixing viewpoint, if the pulsations live longer than τ_k ,

$$\tau_k = 2\pi \left(\frac{d\omega_A}{dx} L_k \right)^{-1}. \quad (34)$$

Of course, we would also require that the pulsation still had a significant amplitude for these effects to be important. These kinetic/two fluid wave modes may broaden the resonance, and will limit the perturbation scales to $\sim L_k$ [*Rankin et al.*, 1993].

To excite equatorial kinetic Alfvén waves, or electron inertia waves above the polar ionosphere, then pulsation length scales must narrow to approximately hundreds of kilometers, $\sim 0.05 - 0.1 R_E$ [see *Rankin et al.*, 1993, and references therein]. For those FLRs with $\tau_k < \tau_I$, then these wave modes will be triggered and consequently we agree with *Inhester* [1987] and *Rankin et al.* [1993] that kinetic/two-fluid waves may be excited within the lifetimes of some long-lived pulsations.

On timescales less than both τ_I and τ_k , then we expect that our ideal MHD code will provide an accurate description of the evolution of a FLR.

5. Conclusions

We have presented an ideal linearised numerical MHD model for the coupling between fast and Alfvén waves in the magnetosphere. Using this model, we examine the temporal evolution of FLR widths driven by fast cavity modes. Three regimes for pulsation evolution become apparent from this analysis.

First, the overall energy width developed by the resonance can be understood in terms of the frequency components of the driving cavity mode. The frequency bandwidth of this mode is governed by its damping rate, and this determines the field lines which are actually being driven. The overall resonance energy width at any time is given by the spatial extent of these driven field lines. This width develops on a timescale $\tau_{fi} = \omega_{fi}^{-1}$ and approaches an asymptotic FWHM of $\Delta\omega_A = 2\omega_{fi}$. This is a new result, which means that at early times the overall energy width of a resonance will be broader than previously thought, and only at large times will it approach the expected asymptotic width.

Second, for perturbations which live longer than τ_{fi} , further fine structure can develop beneath this envelope. Phase mixing between adjacent field lines within the resonance continues to generate finer and finer perturbation scales. Thus the finest possible scales at any time within an ideal magnetospheric pulsation will be governed by the phase mixing length, given by $L_{ph}(t) =$

Table 1. Pulsation Behavior Regimes

Timescales	Energy Width	ξ_y Scale Length	Description
$t < \tau_{fi}, \tau_I, \tau_k$	decreases $\propto t^{-1}$ $\Delta X_E \approx L_{ph}(t)/\sqrt{3}$	decreases $\propto t^{-1}$ $\Delta X_\xi \approx L_{ph}(t)$	no fine structure beneath the energy envelope.
$\tau_{fi} < t < \tau_I, \tau_k$	ΔX_E has saturated $\Delta X_E \approx 2\omega_{fi} (d\omega_A/dx)^{-1}$	decreases $\propto t^{-1}$ $\Delta X_\xi \approx L_{ph}(t)$	ξ_y has fine scale structure within the energy envelope.
$\tau_{fi}, \tau_I < t < \tau_k$	ΔX_E has saturated $\Delta X_E \approx 2\omega_{fi} (d\omega_A/dx)^{-1}$	$\Delta X_\xi \approx L_{ph}(t)$, but its amplitude decays in time	kinetic effects not important. ξ_y amplitude reduces due to ionospheric dissipation.
$\tau_I < t < \tau_k, \tau_{fi}$ $\omega_{fi} \approx 0$ (continually driven)	ΔX_E has saturated $\Delta X_E \sim L_I$	ΔX_ξ has saturated $\Delta X_\xi \approx L_I$.	kinetic effects not important. pulsation maintains dominant scale $\Delta X_\xi \sim L_I$.
$\tau_{fi}, \tau_k < t < \tau_I$	ΔX_E has saturated $\Delta X_E \approx 2\omega_{fi} (d\omega_A/dx)^{-1}$	ΔX_ξ has saturated $\Delta X_\xi \sim L_k$	ξ_y fine structure saturates. pulsation couples to kinetic or two-fluid plasma waves.

$2\pi(t d\omega_A/dx)^{-1}$. If ionospheric dissipation is included, the Alfvén fields will damp exponentially in time as they phase mix.

Third, for the case of continually driven pulsations ($\omega_{fi} \approx 0$), for example driven by a small λ cavity mode, then after a time τ_I the perturbation width will narrow to L_I . At this point the phase mixing process will cease to produce any finer detectable structure within the pulsation, which will appear as a single coherently oscillating wave having width L_I .

If the phase mixing within pulsations can continue for a sufficiently long time, so that it reaches a kinetic/two-fluid scale L_k (by experiencing only slow ionospheric damping), then kinetic/two-fluid effects may also broaden the resonance fine scales and limit them to the order of L_k or more. For various values of τ_{fi} , τ_I , and τ_k , the regimes for pulsation behavior can be summarised as shown in Table 1.

The combination of these features allows pulsation energy envelope widths to be created on the timescale of several cavity mode periods, as observed in data by Walker et al. [1992], and allows the resonances to naturally exhibit the spatially localized packet structure across L shells which is also seen in data [Mitchell et al., 1990; Lin et al., 1992].

We find that pulsations can be expected to exhibit fine structure inside the energy envelope, so long as they are not damped on timescales shorter than τ_{fi} . By considering ionospheric damping as the likely dominant pulsation energy dissipation mechanism, we conclude that for both dayside and active nightside pulsations whose footpoints lie in the auroral region, ionospheric damping can be sufficiently small so that this fine structure is created within the pulsation energy envelope.

Depending on the values of L_{fi} , L_I , and L_k , we agree with both Inhester [1987] and Rankin et al. [1993] that in general it may be possible for some pulsations to live long enough so that sufficiently small scales can develop, and hence that mode conversion to kinetic or two fluid waves should be considered. Both kinetic Alfvén

or electron inertia waves can accelerate particles parallel to the background magnetic field. Hence, it is possible that FLRs have an important role to play in modulating auroral emissions and perhaps in generating some types of auroral arcs [Samson et al., 1991, 1992a; Xu et al., 1993].

Current radar observations show a limiting resolution of ~ 45 km in the ionosphere [Walker et al., 1992]. Thus smaller-scale observations will be necessary to further investigate pulsation fine structure. If the electron precipitation in auroral arcs is in fact a direct result of FLR fields, then, as suggested by Rankin et al. [1993], optical auroral observations might be useful for determining their internal fine structure.

Finally, we note that the MHD code we have employed should be accurate in describing the evolution of pulsations during their growth phase. Only as times of the order of τ_k or τ_I are approached, do kinetic or dissipative effects become important suggesting that the ideal MHD approximation in our model requires revision.

Appendix: Matrix Form of Coupled Equations

Equations (2) and (3) and the half-range Fourier series expansions for ξ_x and ξ_y , yield coupled equations for $a_m(t)$ and $b_m(t)$. With $v_A^{-2}(x) = A^2 - B^2 \cos(\pi x)$, and \ddot{a} denoting $\partial^2 a / \partial t^2$, then

$$-\frac{B^2}{2}\ddot{a}_{m-1}(t) + A^2\ddot{a}_m(t) - \frac{B^2}{2}\ddot{a}_{m+1}(t) + (k_z^2 + (\pi m)^2)a_m(t) + \lambda\pi m b_m(t) = 0 \quad (A1)$$

$$-\frac{B^2}{2}\ddot{b}_{m-1}(t) + A^2\ddot{b}_m(t) - \frac{B^2}{2}\ddot{b}_{m+1}(t) + (k_z^2 + \lambda^2)b_m(t) + \lambda\pi m a_m(t) = 0. \quad (A2)$$

Defining the vector \mathbf{X} as

$$\mathbf{X} = \begin{bmatrix} b_0 \\ a_1 \\ b_1 \\ a_2 \\ b_2 \\ \vdots \end{bmatrix} \quad (\text{A3})$$

and assuming perturbations of the form $e^{-i\omega t}$, (A1) and (A2) can be written as a generalized matrix eigenvalue problem,

$$\omega_n^2 \mathbf{R}^2 \mathbf{X}_{\mathbf{n}} = \mathbf{M} \mathbf{X}_{\mathbf{n}} \quad (\text{A4})$$

where $\mathbf{X}_{\mathbf{n}}$ represents an eigenvector, and ω_n^2 its corresponding eigenvalue. The matrix \mathbf{R}^2 is pentadiagonal and \mathbf{M} is tridiagonal, both being Hermitian.

Truncating the summation to a finite number of Fourier modes, $m = N$, yields for the decoupled ($\lambda = 0$) case N fast modes and $N + 1$ Alfvén modes (i.e., a $(2N + 1)$ by $(2N + 1)$ matrix eigenvalue problem). In general, we can obtain numerically $2N + 1$ eigenfrequencies ω_n^2 , and $2N + 1$ corresponding eigenvectors, representing the coupled wave modes. Writing α_{mn} as the components of a solution matrix, having the solution eigenvectors as its columns, we get a general solution for both $\xi_x(x, t)$ and $\xi_y(x, t)$ in the form

$$\xi_x(x, t) = \sum_{m=1}^N a_m(t) \sin(\pi mx) \quad (\text{A5})$$

where

$$a_m(t) = \sum_{n=1}^{2N+1} \alpha_{m,n} [c_n(t) \cos(\omega_n t) + d_n(t) \sin(\omega_n t)] \quad (\text{A6})$$

and $m_x = 2m$. And similarly,

$$i\xi_y(x, t) = \frac{1}{2} b_0(t) + \sum_{m=1}^N b_m(t) \cos(\pi mx) \quad (\text{A7})$$

where

$$b_0(t) = \sum_{n=1}^{2N+1} \alpha_{1,n} [c_n(t) \cos(\omega_n t) + d_n(t) \sin(\omega_n t)] \quad (\text{A8})$$

$$b_m(t) = \sum_{n=1}^{2N+1} \alpha_{m,y,n} [c_n(t) \cos(\omega_n t) + d_n(t) \sin(\omega_n t)] \quad (\text{A9})$$

where $m_y = 2m + 1$.

The components of the column vectors \mathbf{c} and \mathbf{d} (i.e., c_n and d_n) are determined by the initial conditions at $t = 0$. Hence

$$\alpha \mathbf{c} = \mathbf{e} \quad (\text{A10})$$

$$\alpha \Omega \mathbf{d} = \dot{\mathbf{e}} \quad (\text{A11})$$

where

$$\mathbf{c} = [c_1, c_2, c_3, \dots, c_n]^T \quad (\text{A12})$$

$$\mathbf{d} = [d_1, d_2, d_3, \dots, d_n]^T \quad (\text{A13})$$

$$\Omega = \text{diag}[\omega_1, \omega_2, \omega_3, \dots, \omega_n] \quad (\text{A14})$$

$$\mathbf{e} = [b_0(t=0), a_1(t=0), b_1(t=0), \dots, a_n(t=0), b_n(t=0)]^T \quad (\text{A15})$$

$$\dot{\mathbf{e}} = [\dot{b}_0(t=0), \dot{a}_1(t=0), \dot{b}_1(t=0), \dots, \dot{a}_n(t=0), \dot{b}_n(t=0)]^T \quad (\text{A16})$$

The summations for ξ_x and ξ_y , can also be written in terms of a sum over spatial modes. We can write,

$$\xi_x(x, t) = \sum_{n=1}^{2N+1} [c_n(t) \cos(\omega_n t) + d_n(t) \sin(\omega_n t)] \phi_{nx}(x) \quad (\text{A17})$$

where $\phi_{nx}(x)$ is the spatial variation of the mode in the \hat{x} direction given by

$$\phi_{nx}(x) = \sum_{m=1}^N \alpha_{m,n} \sin(\pi mx) \quad (\text{A18})$$

$(m_x = 2m)$

$$i\xi_y(x, t) = \sum_{n=1}^{2N+1} [c_n(t) \cos(\omega_n t) + d_n(t) \sin(\omega_n t)] \phi_{ny}(x) \quad (\text{A19})$$

where

$$\phi_{ny}(x) = \alpha_{1,n} + \sum_{m=1}^N \alpha_{m,y,n} \cos(\pi mx) \quad (\text{A20})$$

$(m_y = 2m + 1)$.

The functions $\phi_{nx}(x)$ and $\phi_{ny}(x)$ each have a time dependence of $e^{\pm i\omega_n t}$; thus they are normal modes (in the generalized function sense). In fact, they represent a Fourier approximation to the Barston modes of the system [Cally, 1991].

We should also note that for coupled modes, both sets of spatial modes $\phi_{nx}(x)$ and $\phi_{ny}(x)$ exist for all values of n from 1 to $(2N + 1)$. Within our numerical scheme, the decoupled ($\lambda = 0$) structure of a mode with n corresponding to either a fast or an Alfvén mode, leaves a dominant component in either $\phi_{nx}(x)$ or $\phi_{ny}(x)$, respectively. For this $\lambda = 0$ case, the amplitude in the perpendicular polarisation is zero, except for computer round-off error. Clearly, when $\lambda \neq 0$, then both polarizations become important for both fast and Alfvén modes.

Acknowledgments. This work was carried out while I.R.M. was supported by a PPARC studentship, and A.N.W. was supported by a PPARC Advanced Fellowship.

The Editor thanks P. J. Cargill and R. E. Denton for their assistance in evaluating this paper.

References

- Allan, W., and E. M. Poulter, Damping of magnetospheric cavity modes: A discussion, *J. Geophys. Res.*, **94**, 11,843, 1989.
- Allan, W., S. P. White, and E. M. Poulter, Impulse-excited hydromagnetic cavity and field-line resonances in the magnetosphere, *Planet. Space Sci.*, **34**, 371, 1986a.
- Allan, W., E. M. Poulter, and S. P. White, Hydromagnetic wave coupling in the magnetosphere - plasmapause effects on impulse-excited resonances, *Planet. Space Sci.*, **34**, 1189, 1986b.
- Anderson, B. J., M. J. Engebretson, and L. J. Zanetti, Distortion effects in spacecraft observations of MHD toroidal standing waves: Theory and observations, *J. Geophys. Res.*, **94**, 13,425, 1989.
- Barston, E. M., Electrostatic oscillations in inhomogeneous cold plasmas, *Ann. Phys. N.Y.*, **29**, 282, 1964.
- Boyd, T. J. N., and J. J. Sanderson, *Plasma Dynamics*, Nelson, London, 1969.
- Bracewell, R. N., *The Fourier Transform and Its Applications*, McGraw-Hill, New York, 1978.
- Bray, R. J., and R. E. Loughhead, *The Solar Chromosphere*, Chapman and Hall, London, 1974.
- Browning, P. K., and E. R. Priest, Kelvin-Helmholtz instability of a phase-mixed Alfvén wave, *Astron. Astrophys.*, **131**, 283, 1984.
- Budden, K. G., *Radio Waves in the Ionosphere*, Cambridge Univ. Press., New York, 1961.
- Burghes, D. N., P. C. Kendall, and P. A. Sweet, A Physical explanation of the difficulties appearing in the theory of toroidal magnetohydrodynamic oscillations, *Mon. Not. R. Astron. Soc.*, **143**, 9, 1969.
- Cally, P. S., Phase mixing and surface waves : A new interpretation, *J. Plasma Phys.*, **45**, 453, 1991.
- Cally, P. S., and Z. Sedláček, A Fourier-space description of oscillations in an inhomogeneous plasma, II, Discrete approach, *J. Plasma Phys.*, **52**, 265, 1994.
- Chen, L., and A. Hasegawa, A theory of long-period magnetic pulsations, I, Steady state excitation of field line resonance, *J. Geophys. Res.*, **79**, 1024, 1974.
- Crowley, G., W. J. Hughes, and T. B. Jones, Observational evidence for cavity modes in the Earth's magnetosphere, *J. Geophys. Res.*, **92**, 12,233, 1987.
- Dungey, J. W., Electrodynamics of the outer atmosphere, *Sci. Rep.* **69**, Penn. State Univ., Univ. Park, Pa., 1954.
- Dungey, J. W., Hydromagnetic waves, in *Physics of Geomagnetic Phenomena*, vol. 2, edited by S. Matsushita and W. H. Campbell, p.913, Academic, San Diego, Calif., 1967.
- Ellis, P., and D. J. Southwood, Reflection of Alfvén waves by non-uniform ionospheres, *Planet. Space Sci.*, **31**, 107, 1983.
- Forslund, D., J. M. Kindel, K. Lee, E. L. Lindman, and R. L. Morse, Theory and simulation of absorption in a hot plasma, *Phys. Rev. A*, **11**, 679, 1975.
- Harrold, B. G., and J. C. Samson, Standing ULF modes of the magnetosphere: A theory, *Geophys. Res. Lett.*, **19**, 1811, 1992.
- Heyvaerts, J., and E. R. Priest, Coronal heating by phase mixed shear Alfvén waves, *Astron. Astrophys.*, **117**, 220, 1983.
- Hughes, W. J., Hydromagnetic waves in the magnetosphere, in *Solar Terrestrial Physics - Principles and Theoretical Foundations*, edited by R. L. Carvillano and J. M. Forbes, p.453, D. Reidel, Norwell, Mass., 1983.
- Hughes, W. J., Magnetospheric ULF waves: A tutorial with a historical perspective, in *Solar Wind Sources of Magne-*
- tospheric Ultra-Low-Frequency Waves, Geophys. Monogr.* ser., vol. 81, edited by M. J. Engebretson, K. Takahashi, and M. Scholer, p.1, AGU, Washington, D.C., 1994.
- Inhester, B., Numerical modelling of hydromagnetic wave coupling in the magnetosphere, *J. Geophys. Res.*, **92**, 4751, 1987.
- Kivelson, M. G., and D. J. Southwood, Resonant ULF waves: A new interpretation, *Geophys. Res. Lett.*, **12**, 49, 1985.
- Kivelson, M. G., and D. J. Southwood, Coupling of global magnetospheric MHD eigenmodes to field line resonances, *J. Geophys. Res.*, **91**, 4345, 1986.
- Kivelson, M. G., and D. J. Southwood, Hydromagnetic waves and the ionosphere, *Geophys. Res. Lett.*, **15**, 1271, 1988.
- Kivelson, M. G., J. Etcheto, and J. G. Trotignon, Global compressional oscillations of the Terrestrial magnetosphere: The evidence and a model, *J. Geophys. Res.*, **89**, 9851, 1984.
- Lee, D. H., and R. L. Lysak, Magnetospheric ULF wave coupling in the dipole model: The impulsive excitation, *J. Geophys. Res.*, **91**, 17,097, 1989.
- Lin, N., M. J. Engebretson, L. A. Reinleitner, J. V. Olson, D. L. Gallagher, L. J. Cahill Jr, J. A. Slavin, and A. M. Persoon, Field and thermal plasma observations of ULF pulsations during a magnetically disturbed interval, *J. Geophys. Res.*, **97**, 14,859, 1992.
- McLachlan, N. W., *Theory and Application of Mathieu Functions*, Oxford University Press, Oxford, 1947.
- Mitchell, D. G., M. J. Engebretson, D. J. Williams, C. A. Cattell, and R. Lundin, Pc 5 pulsations in the outer dawn magnetosphere seen by ISEE 1 and 2, *J. Geophys. Res.*, **95**, 967, 1990.
- Newton, R. S., D. J. Southwood, and W. J. Hughes, Damping of geomagnetic pulsations by the ionosphere, *Planet. Space Sci.*, **26**, 201, 1978.
- Poedts, S., M. Goossens, and W. Kerner, Temporal evolution of resonant absorption in solar coronal loops, *Comp. Phys. Comm.*, **59**, 95, 1990.
- Radoski, H. R., A theory of latitude dependent geomagnetic micropulsations: The asymptotic fields, *J. Geophys. Res.*, **79**, 595, 1974.
- Radoski, H. R., Hydromagnetic waves: Temporal development of coupled modes, *Environ. Res. Pap.* **559**, Air Force Geophys. Lab., Hanscom Air Force Base, Mass., 1976.
- Rankin, R., J. C. Samson, and P. Frycz, Simulations of driven field line resonances in the Earth's magnetosphere, *J. Geophys. Res.*, **98**, 21,341, 1993.
- Rickard, G. J., and A. N. Wright, Alfvén resonance excitation and fast wave propagation in magnetospheric waveguides, *J. Geophys. Res.*, **99**, 13,455, 1994.
- Rickard, G. J., and A. N. Wright, ULF pulsations in a magnetospheric waveguide: Comparison of real and simulated satellite data, *J. Geophys. Res.*, **100**, 3531, 1995.
- Ruohoniemi, J. M., R. A. Greenwald, K. B. Baker, and J. C. Samson, HF radar observations of field line resonances in the midnight/early morning sector, *J. Geophys. Res.*, **96**, 15,697, 1991.
- Samson, J. C., T. J. Hughes, F. Creutzberg, D. D. Wallis, R. A. Greenwald, and J. M. Ruohoniemi, Observations of a detached, discrete arc in association with field line resonances, *J. Geophys. Res.*, **96**, 15,683, 1991.
- Samson, J. C., D. D. Wallis, T. J. Hughes, F. Creutzberg, J. M. Ruohoniemi, and R. A. Greenwald, Substorm intensifications and field line resonances in the nightside magnetosphere, *J. Geophys. Res.*, **97**, 8495, 1992a.
- Samson, J. C., B. G. Harrold, J. M. Ruohoniemi, and A. D. M. Walker, Field line resonances associated with

- MHD waveguides in the magnetosphere, *Geophys. Res. Lett.*, **19**, 441, 1992b.
- Sedláček, Z., Electrostatic oscillations in a cold inhomogeneous plasma, I, Differential equation approach, *J. Plasma Phys.*, **5**, 239, 1971.
- Southwood, D. J., Some features of field line resonances in the magnetosphere, *Planet. Space Sci.*, **22**, 483, 1974.
- Southwood, D. J., and W. J. Hughes, Theory of hydromagnetic waves in the magnetosphere, *Space Sci. Rev.*, **35**, 301, 1983.
- Southwood, D. J., and W. Allan, Hydromagnetic cavity eigenmodes in a non-uniform plasma, *Proceedings of 21st ESLAB Symposium (Small Scale Plasma Processes)*, Eur. Space Agency Spec. Publ., ESA SP-275, 179, 1987.
- Steinolfson, R. S. and J. M. Davila, Coronal heating by resonant absorption of Alfvén waves: The importance of the global mode and scaling laws, *Ap. J.*, **415**, 354, 1993.
- Walker, A. D. M., R. A. Greenwald, W. F. Stewart, and C. A. Green, Stare auroral radar observations of Pc 5 geomagnetic pulsations, *J. Geophys. Res.*, **84**, 3373, 1979.
- Walker, A. D. M., J. M. Ruohoniemi, K. B. Baker, and R. A. Greenwald, Spatial and temporal behaviour of ULF pulsations observed by the Goose Bay HF radar, *J. Geophys. Res.*, **97**, 12,187, 1992.
- Wright, A. N., Coupling of fast and Alfvén modes in realistic magnetospheric geometries, *J. Geophys. Res.*, **97**, 6429, 1992a.
- Wright, A. N., Asymptotic and time-dependent solutions of magnetic pulsations in realistic magnetic field geometries, *J. Geophys. Res.*, **97**, 6439, 1992b.
- Wright, A. N., Dispersion and wave coupling in inhomogeneous MHD waveguides, *J. Geophys. Res.*, **99**, 159, 1994a.
- Wright, A. N., MHD theory of magnetic pulsations, in *Physical Signatures of Magnetospheric Boundary Layer Processes*, edited by J. A. Holtet and A. Egeland, p. 329, Kluwer Academic, Norwell Mass., 1994b.
- Xu, B. L., J. C. Samson, W. W. Liu, F. Creutzberg, and T. J. Hughes, Observations of optical Aurora modulated by resonant Alfvén waves, *J. Geophys. Res.*, **98**, 11,531, 1993.
- Zhu, X., and M. G. Kivelson, Analytic formulation and quantitative solutions of the coupled ULF wave problem, *J. Geophys. Res.*, **93**, 8602, 1988.
- Zhu, X., and M. G. Kivelson, Global mode pulsations in a magnetosphere with a non-monotonic Alfvén velocity profile, *J. Geophys. Res.*, **94**, 1479, 1989.
- Ziesolleck, C. W. S., B. J. Fraser, F. W. Menk, and P. W. McNabb, Spatial characteristics of low-latitude Pc3-4 geomagnetic pulsations, *J. Geophys. Res.*, **98**, 197, 1993.
-
- P. S. Cally, Department of Mathematics, Monash University, Clayton, Victoria 3168, Australia. (e-mail: cally@zeus.maths.monash.edu.au)
- Ian R. Mann, Andrew N. Wright, Department of Mathematical and Computational Sciences, University of St. Andrews, Fife, Scotland, KY16 9SS. (e-mail: ianm@dcs.st-and.ac.uk; andy@dcs.st-and.ac.uk)

(Received January 5, 1995; revised March 8, 1995; accepted March 9, 1995.)